


Published: 05 March 2018

## A Fuzzy Inventory Model for a Deteriorating Item with Variable Demand, Permissible Delay in Payments and Partial Backlogging with Shortage Follows Inventory (SFI) Policy

Ali Akbar Shaikh, [Asoke Kumar Bhunia](#), [Leopoldo Eduardo Cárdenas-Barrón](#) , [Laxminarayan Sahoo](#) & [Sunil Tiwari](#)


*International Journal of Fuzzy Systems* **20**, 1606–1623 (2018)

181 Accesses | 25 Citations | [Metrics](#)

### Abstract

This research studies a fuzzy inventory model for a deteriorating item with permissible delay in payments. For this paper, the demand depends on selling price and the frequency of the advertisement. In order to make a more realistic inventory model, it is considered the case of stock-out which is partial backlogged. In this work, it is taken account the shortage follows inventory (SFI) policy. Several scenarios and sub-scenarios have been provided, and each corresponding problem has been defined as a constrained optimization problem in the fuzzy environment. Further, these problems have converted into a new problem using the nearest interval approximation technique of fuzzy numbers.

## Optimal Redundancy Allocation for Bridge Network System with Fuzzy Parameters

 [Pdf Version](#)

[Laxminarayan SAHOO](#)  
[Sanat Kumar MAHATO](#)

### Keywords

[Redundancy allocation](#), [Bridge network system](#), [Genetic Algorithm](#), [Fuzzy parameter](#), [Defuzzification](#), [Statistical Beta Distribution](#)

### Abstract

The goal of this paper is to formulate and solve the redundancy allocation problem with fuzzy parameters as a non-convex integer nonlinear constrained optimization problem. Here, redundancy allocation problem of bridge network system with fuzzy parameters has been considered and its solution methodology has been proposed. The solution methodology is based on defuzzification of fuzzy parametric values and use of real coded genetic algorithm. Here, a new defuzzification technique based on statistical Beta distribution has been used for defuzzification. For solving the constrained optimization problems, we have used genetic algorithm based penalty function technique. Finally, a numerical example has been presented for illustration purpose.

[\(top\)](#)  
[\(back to issue\)](#)

Copyright © JAQM, 2018. All Rights Reserved. [Terms of use](#)

## Slow fission of highly excited plutonium nuclei

A. K. Sikdar,<sup>1</sup> A. Ray,<sup>1\*</sup> Deepak Pandit,<sup>1</sup> B. Dey,<sup>1</sup> Sarmishtha Bhattacharyya,<sup>1</sup> Soumik Bhattacharyya,<sup>1</sup> A. Bisoi,<sup>2,1</sup> A. De,<sup>3</sup> S. Paul,<sup>3</sup> Srijit Bhattacharya,<sup>4</sup> and A. Chatterjee<sup>5</sup>

<sup>1</sup>Variable Energy Cyclotron Centre, 1/AF Bidhannagar, Kolkata 700064, India

<sup>2</sup>Saha Institute of Nuclear Physics, 1/AF Bidhannagar, Kolkata 700064, India

<sup>3</sup>Raniganj Girls' College, Raniganj 713358, West Bengal, India

<sup>4</sup>Department of Physics, Barasat Govt. College, Kolkata 700124, India

<sup>5</sup>Inter-University Accelerator Center, New Delhi 110067, India

(Received 18 February 2017; revised manuscript received 5 February 2018; published 14 August 2018)

**Background:** Earlier measurements of fission lifetimes of the highly excited uraniumlike nuclei by  $K$  x-ray fluorescence and crystal blocking techniques obtained slow fission (fission time  $\sim 10^{-18}$  s) for most of the fission events and were shown to be incompatible with the very short fission time ( $\sim 10^{-20}$  s) obtained by the nuclear techniques and also with the very small ( $\leq 5\%$ ) percentage of such slow fission events predicted by simple statistical models. One weakness of the earlier fluorescence experiments is that the observed  $K$  x-ray peaks were very broad [full width at half maximum (FWHM)  $\approx 15$  keV] and the precise energies of the relevant  $K$  x-ray lines could not be determined from such measurements.

**Purpose:** The purpose is to look at the relevant  $K$  x-ray energy region in coincidence with the fission fragments with a high resolution ( $\approx 1$  keV) spectrometer to obtain evidence of slow fission and determine its percentage.

**Method:** Highly excited plutonium nuclei were produced in the fusion of  $^4\text{He} + ^{238}\text{U}$  at  $E(^4\text{He})_{\text{lab}} = 60$  MeV. The intrinsic width of plutonium  $K$  x-ray lines in coincidence with the fission fragments was determined as a direct measure (or lower limit) of the fission time of the slow ( $\sim 10^{-18}$  s) fission events. The minimum percentage of slow fission events has been determined from the  $K$  x-ray multiplicity per fission event and the probability of creation of  $K$ -orbital vacancies in plutonium.

**Results:** A narrow peak (FWHM  $\approx 1$  keV) observed in the coincidence photon spectrum at  $(102.8 \pm 0.5)$  keV, just below the characteristic plutonium  $K_{\alpha 1}$  line (103.7 keV) has been attributed to the plutonium  $K_{\alpha 1}$  line on the basis of supporting evidence and calculations and we deduce that most of the fission events are slow (fission time  $> 10^{-18}$  s). No peak has been observed exactly at 103.7 keV.

**Conclusions:** The shift  $(0.9 \pm 0.5)$  keV of plutonium  $K$  x-ray lines is plausible, if the fissioning plutonium nucleus spends most of its long fission time in a highly deformed dumbbell shape (beyond saddle) and the corresponding results are in agreement with those obtained earlier by the atomic techniques. Alternatively, if no significant shift of plutonium  $K$  x-ray lines can be expected, the absence of a peak at 103.7 keV contradicts earlier atomic technique claims of a significant percentage of slow fission events.

DOI: 10.1103/PhysRevC.98.024615

### I. INTRODUCTION

Nuclear fission is one of the most important discoveries of the 20th century and in this context, the fission dynamics of highly excited fissile nuclei has a special significance. The time scale of the nuclear fission process of highly excited fissile nuclei is a basic characteristic of the underlying fission dynamics. However, atomic techniques ( $K$  x-ray-fission fragment coincidence and crystal blocking techniques) [1–6] have deduced long fission times ( $\sim 10^{-18}$  s) for most of the fission events of highly excited fissile nuclei, whereas nuclear techniques and calculations [7–11] have obtained much

shorter fission time ( $\sim 10^{-20}$  s). Both the nuclear and atomic techniques are sensitive to the time that elapses between the formation of the fissioning nucleus to its scission. This time is generally called the fission time. Hereinafter, we distinguish two fission lifetime ranges: fission lifetimes  $> 10^{-18}$  s will be referred to as long fission time or slow fission events and fission lifetimes  $< 10^{-19}$  s will be referred to as short fission time. Bulgac *et al.* [11] performed fission dynamics calculations using a density functional technique and obtained short saddle to scission times for excited ( $E_x = 8$  MeV)  $^{240}\text{Pu}$  nuclei. A distribution of fission times stretching to very long fission time scales has been obtained from Langevin fluctuation-dissipation dynamical calculations [12,13] and the percentage of fission events having long fission times could be increased arbitrarily by increasing the viscosity parameter. The vastly different fission time scales as deduced from the nuclear and atomic techniques have been attributed to the sensitivity of the techniques to different time domains [12,13]. It was argued

\*Corresponding authors: ray@vecc.gov.in; amlanray2016@gmail.com

<sup>1</sup>Present Address: Department of Physics, Indian Institute of Engineering Science and Technology, Shibpur, Howrah 711103, India.

Alok Kumar De





## Study of giant dipole resonance in hot rotating light mass nucleus $^{31}\text{P}$



Debasish Mondal<sup>a,\*</sup>, Deepak Pandit<sup>a</sup>, S. Mukhopadhyay<sup>a,b</sup>, Surajit Pal<sup>a</sup>,  
Srijit Bhattacharya<sup>c</sup>, A. De<sup>d</sup>, N. Dinh Dang<sup>e,f</sup>, N. Quang Hung<sup>g</sup>, Soumik Bhattacharya<sup>a,b</sup>,  
S. Bhattacharyya<sup>a,b</sup>, Balaram Dey<sup>h</sup>, Pratap Roy<sup>a</sup>, K. Banerjee<sup>a,b,i</sup>, S.R. Banerjee<sup>i</sup>

<sup>a</sup> Variable Energy Cyclotron Centre, 1/AF-Bidhannagar, Kolkata 700064, India

<sup>b</sup> Homi Bhabha National Institute, Training School Complex, Anushaktinagar, Mumbai 400094, India

<sup>c</sup> Department of Physics, Barasat Government College, Kolkata 700124, India

<sup>d</sup> Department of Physics, Ramganga Girls' College, Ramganga 713358, India

<sup>e</sup> Quantum Hadron Physics Laboratory, RIKEN Nishina Center for Accelerator-Based Science, RIKEN, 2-1 Hirosawa, Wako City, Saitama 351-0198, Japan

<sup>f</sup> Institute of Nuclear Science and Technique, Hanoi 122100, Vietnam

<sup>g</sup> Institute of Fundamental and Applied Sciences, Duy Tan University, Ho Chi Minh City 700000, Vietnam

<sup>h</sup> Saha Institute of Nuclear Physics, 1/AF-Bidhannagar, Kolkata 700064, India

<sup>i</sup> Variable Energy Cyclotron Centre, 1/AF-Bidhannagar, Kolkata 700064, India

### ARTICLE INFO

#### Article history:

Received 21 May 2018

Received in revised form 3 July 2018

Accepted 27 July 2018

Available online 30 July 2018

Editor: V. Metag

#### Keywords:

Isovector giant dipole resonance  
Statistical theory of nucleus  
NaF<sub>2</sub> detectors

### ABSTRACT

An exclusive systematic study of the giant dipole resonance (GDR) parameters has been performed in very light mass nucleus  $^{31}\text{P}$  in the temperature range of  $\sim 0.8$ – $2.1$  MeV and average angular momentum of  $\sim 11$ – $16$   $\hbar$ . The high-energy  $\gamma$  rays from the decay of the GDR, evaporated neutrons and  $\gamma$ -ray multiplicities have been measured. The angular distribution of high-energy  $\gamma$  rays has also been measured at  $E_{\text{beam}} = 42$  MeV. The GDR parameters, nuclear level density parameter and nuclear temperature were precisely determined by simultaneous statistical model analysis of high-energy  $\gamma$  ray and evaporated neutron spectra. It is observed that the measured width remains roughly constant up to a temperature of  $\sim 1.6$  MeV. Moreover, the thermal pairing plays no role in describing the GDR width in this open-shell light nucleus at the above-mentioned temperatures and angular momenta. The present measurements provide an excellent platform to extend the applicability of the existing theoretical models down to the very light mass nuclei.

© 2018 The Authors. Published by Elsevier B.V. This is an open access article under the CC BY license (<http://creativecommons.org/licenses/by/4.0/>). Funded by SCOAP<sup>2</sup>.

The isovector giant dipole resonance (IVGDR or commonly known as GDR) is a member of a broad family of collective resonances in nuclei called giant resonances [1,2]. Macroscopically, it is conceived as the out-of-phase oscillation of proton and neutron fluids, while microscopically, it is described as the coherent excitation of 1 particle–1 hole (1p–1h) configurations across one major shell. The short lifetime of this resonance makes it an excellent probe to study the nuclear properties at extreme conditions, e.g. nuclear shapes and deformations at high temperature and angular momentum [3–10], fission time scale [11–13], isospin mixing [14–20], the ratio of nuclear shear viscosity to entropy volume density [21,22] etc.

#### \* Corresponding author.

E-mail address: [debasishm@vecc.gov.in](mailto:debasishm@vecc.gov.in) (D. Mondal).

<sup>†</sup> Present address: Department of Nuclear Physics, Research School of Physics and Engineering, The Australian National University, ACT0200, Australia.

<https://doi.org/10.1016/j.physletb.2018.07.057>

0370-2693/© 2018 The Authors. Published by Elsevier B.V. This is an open access article under the CC BY license (<http://creativecommons.org/licenses/by/4.0/>). Funded by SCOAP<sup>2</sup>.

Alok Kumar De

After the first observation of the GDR built on the nuclear excited states in heavy-ion fusion reactions nearly four decades ago [23], a great wealth of data has been accumulated over the years regarding the properties of the GDR parameters [1,24–27]. It is observed that the GDR energy remains roughly constant at the ground-state value with increasing nuclear temperature ( $T$ ) and angular momentum ( $J$ ), while the width increases with both  $T$  and  $J$ . It is worth mentioning, in this context, that in a heavy-ion fusion reaction, the compound nucleus (CN) is populated at high  $J$  along with the intrinsic excitation. It is, therefore, very difficult to disentangle the effects of  $T$  and  $J$  on the GDR width. Researchers have also used inelastic scattering to study the GDR [28–30]. In this case, the CN is populated at low angular momentum but with a broad range of excitation energy. Another excellent technique to study the exclusive temperature dependence of the GDR is using the light-ion induced fusion reaction, in which the CN is populated at a definite initial excitation energy and a small distribution of  $J$  as compared to that obtained in the heavy-ion

## Experimental signature of collective enhancement in nuclear level density

Deepak Pandit,<sup>1,2</sup> Srijit Bhattacharya,<sup>2</sup> Debasish Mondal,<sup>1,3</sup> Pratap Roy,<sup>1,3</sup> K. Banerjee,<sup>1,3,4</sup> S. Mukhopadhyay,<sup>1,3</sup> Surajit Pal,<sup>1</sup> A. De,<sup>4</sup> Balaram Dey,<sup>5</sup> and S. R. Banerjee<sup>6</sup><sup>1</sup>Variable Energy Cyclotron Centre, IIAF-Bidhannagar, Kolkata 700064, India<sup>2</sup>Department of Physics, Barasat Government College, Barasat, N 24 Pgs. Kolkata 700124, India<sup>3</sup>Homi Bhabha National Institute, Training School Complex, Anushaktinagar, Mumbai 400094, India<sup>4</sup>Department of Physics, Raniganj Girls' College, Raniganj 713358, India<sup>5</sup>Saha Institute of Nuclear Physics, IIAF-Bidhannagar, Kolkata 700064, India<sup>6</sup>(Ex)Variable Energy Cyclotron Centre, IIAF-Bidhannagar, Kolkata 700064, India

✉ (Received 12 October 2017; published 3 April 2018)

We present a probable experimental signature of collective enhancement in the nuclear level density (NLD) by measuring the neutron and the giant dipole resonance (GDR)  $\gamma$  rays emitted from the rare-earth  $^{160}\text{Tm}$  compound nucleus populated at 26.1 MeV excitation energy. An enhanced yield is observed in both neutron and  $\gamma$ -ray spectra corresponding to the same excitation energy in the daughter nuclei. The enhancement could only be reproduced by including a collective enhancement factor in the Fermi gas model of NLD to explain the neutron and GDR spectra simultaneously. The experimental results show that the relative enhancement factor is of the order of 10 and the fadeout occurs at  $\sim 14$  MeV excitation energy, much before the commonly accepted transition from deformed to spherical shape. We also explain how the collective enhancement contribution changes the inverse level density parameter  $k$  from 8 to 9.5 MeV observed recently in several deformed nuclei.

DOI: 10.1103/PhysRevC.97.041301

The atom, consisting of a tiny nucleus of protons and neutrons surrounded by a cloud of electrons, is responsible for nearly all the properties of matter that have shaped the world around us. Although the atomic properties are governed by the electronic structure, its existence is decided by the nucleus. It is a complex quantal system which is held together by a strong nuclear force. The nucleus attains a variety of configurations even if a small excitation energy is provided to it. The density of nuclear levels increases rapidly with increasing excitation energy [1,2]. Thus, statistical models are not only appropriate but also essential for the comprehension and prediction of different modes of nuclear decay at moderate and high excitation energies. One of the important ingredients of the statistical model is the nuclear level density (NLD) which is defined as the number of excited levels per unit of excitation energy. The NLD has an important contribution in the calculations of explosive nuclear burning in astrophysical environments such as nuclear reaction rates in nucleosynthesis and reliable estimates of nuclear abundance [3,4] as well as in nuclear fission [5], multifragmentation [6], and spallation reactions [7]. It also provides important information about the nuclear thermodynamic properties such as temperature  $T$ , entropy, and heat capacity [8]. The NLD is extracted experimentally by counting the levels, neutron resonance studies [9], Oslo technique [10], two-step cascade method [11],  $\beta$ -Oslo method [12],

$\gamma$ -ray calorimetry [13], and particle evaporation spectra [14]. Theoretically, it has been characterized by phenomenological analytical expressions [1,15,16] as well as calculations based on different microscopic approaches [17–20].

Apart from the intrinsic excitation, the nucleus also displays collective vibrational and rotational motion analogous to atomic and molecular physics. These collective degrees of freedom introduce new levels up to moderate excitation energies, and their contribution is described as the collective enhancement factor in the NLD. The contribution of collectivity in the NLD  $\rho(E^*, J)$  at excitation energy  $E^*$  and angular momentum  $J$  is expressed phenomenologically [15] as

$$\rho(E^*, J) = \rho_{\text{int}}(E^*, J) * K_{\text{coll}}, \quad (1)$$

where  $\rho_{\text{int}}(E^*, J)$  is the intrinsic single-particle level density and  $K_{\text{coll}}$  is the collective enhancement factor. Although the NLD is indispensable in the study of nuclear decay, the collective enhancement in the NLD is still not a well understood topic due to the lack of experimental data. The magnitude and exact form of  $K_{\text{coll}}$  still remains an open question. Several expressions for  $K_{\text{coll}}$  exist in literature where the degree of enhancement varies from 10 to 100 [19,21–23]. On the other hand, the earlier experimental studies have produced contradictory results on the collective enhancement and its fadeout [23,24]. Quite recently, our extensive studies on neutron evaporation from several deformed nuclei have established the fact that the fadeout of collectivity is related to the nuclear shape phase transition and occurs at an excitation energy in the region of 14–21 MeV [25,26]. While a sharp change in the value of inverse level density parameter  $k$ , within the initial compound nuclear excitation energy interval

<sup>\*</sup>deepak.pandit@vecc.gov.in<sup>†</sup>Present address: Department of Nuclear Physics, Research School of Physics and Engineering, Australian National University, Canberra, ACT 2601, Australia.Alok Kumar *et al.*



HYPOTHESIS



# Bone marrow stem cells to destroy circulating HIV: a hypothetical therapeutic strategy

Umesh Chandra Halder\*

## Abstract

Human immunodeficiency virus (HIV) still poses enigmatic threats to human life. This virus has mastered in bypassing anti retroviral therapy leading to patients' death. Circulating viruses are phenomenal for the disease outcome. This hypothesis proposes a therapeutic strategy utilizing receptor-integrated hematopoietic, erythroid and red blood cells. Here, HIV specific receptors trap circulating viruses that enter erythrocyte cytoplasm and form inactive integration complex. This model depicts easy, effective removal of circulating HIV without any adverse effect.

**Keywords:** HIV, AIDS, HIV therapy, Hematopoietic stem cell, Red blood cell, HIV receptors, Burst-forming unit-erythrocyte

## Background

Having around 36 years of understanding after its discovery [1], scientists are still haunting a full and effective cure for human immunodeficiency virus (HIV) and its outcome acquired immunodeficiency syndrome (AIDS). Till date thousands of research efforts have revealed plethora of information regarding its life cycle [2–8] that characterized enigmatic AIDS. These immense knowledge provided possible targets for AIDS therapy [3–5, 8–11] that intervene entry, replication, packaging or budding of the virus leading to anti-retroviral therapy (ART) [12–17]. Apart from having diverse side-effects, ART has certain limitations too, as it only delays patients' death but does not cure AIDS and also it only targets replicating HIVs and not the latent viral particles. Moreover, in doing so, it evokes successive immune compromising reactions making the situation worse. Circulating replicative HIV remains the biggest threat toward successful AIDS therapy. Therefore, an effective strategy is essential that can confer resistance towards circulating HIV particles. If replicating HIV particles were somehow eliminated, it would greatly reduce the effective viral burden

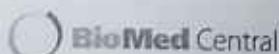
from human body. On the other hand, latency provide base for long term existence of HIV without eliciting any immune response hiding deep inside immune organs [18–20]. Very recently, other than anti-retroviral drugs, such as experimentally promising HIV vaccine [21], neutralizing antibodies [22–24] and Clustered regularly interspaced short palindromic repeat-CRISPR-associated protein-9 nuclease (CRISPR-Cas 9) have shown effectiveness against HIV [25, 26] with certain limitations [27].

The most fascinating event in the viral life cycle is that only a few viral proteins effectively control and direct the cellular pathways for their own sake. So, knowledge of viral proteins functioning in the virus life cycle and properly targeting them may confer successful elimination of HIV from human body.

## Hypothesis


Previously transgenic mice showed effectiveness against Coxsackie virus B infection [28]. Here in this hypothesis, a therapeutic strategy has been proposed for AIDS treatment that would utilize bone marrow stem cells. The proposed therapeutic strategy exploits receptor-integrated red blood corpuscles (riRBC) to trap and finally kill the circulating HIVs. According to this model, RBC membranes can be loaded with cluster of differentiation 4 (CD4) receptor along with C-C chemokine receptor

\*Correspondence: umeshchandrahalder@gmail.com  
Department of Zoology, Ranigang Girls' College, Seansole, Rajbari,  
Ranigang, Paschim Bardhaman, West Bengal 713358, India



© The Author(s) 2018. This article is distributed under the terms of the Creative Commons Attribution 4.0 International License (<http://creativecommons.org/licenses/by/4.0/>), which permits unrestricted use, distribution, and reproduction in any medium, provided you give appropriate credit to the original author(s) and the source, provide a link to the Creative Commons license, and indicate if changes were made. The Creative Commons Public Domain Dedication waiver (<http://creativecommons.org/publicdomain/zero/1.0/>) applies to the data made available in this article, unless otherwise stated.

# Estrogen-regulated expression of P450arom genes in the brain and ovaries of adult female Indian climbing perch, *Anabas testudineus*

Puja Pal<sup>1,3\*</sup> | Sujata Roy Moulik<sup>2,3\*</sup> | Shreyasi Gupta<sup>3</sup> | Payel Guha<sup>3</sup> |  
Suravi Majumder<sup>3</sup> | Sourav Kundu<sup>4</sup> | Buddhadev Mallick<sup>3</sup> | Kousik Pramanick<sup>5</sup> |  
Dilip Mukherjee<sup>3</sup> 

<sup>1</sup>Department of Zoology, Taki Government College, Taki, India

<sup>2</sup>Department of Zoology, Chandernagore College, Chandernagore, India

<sup>3</sup>Endocrinology Laboratory, Department of Zoology, University of Kalyani, Kalyani, India

<sup>4</sup>Department of Botany, West Bengal State University, Barasat, India

<sup>5</sup>Department of Zoology, Presidency University, Kolkata, India

## Correspondence

Prof. Dilip Mukherjee, Department of Zoology, University of Kalyani, PO: Kalyani, Dist: Nadia, WB-741235.

Email: dilipmukher@rediffmail.com

## Funding information

Science and Engineering Research Board

\*Both authors contributed equally to this work.

## Abstract

Cytochrome P450arom (CYP19), a product of *cyp19a1* gene, catalyzes the conversion of androgens to estrogens and is essential for regulation of reproductive function in vertebrates. In the present study, we isolated partial cDNA encoding the ovarian (*cyp19a1a*) and brain (*cyp19a1b*) P450arom genes from adult female perch, *Anabas testudineus* and investigated their regulation by estrogen in vivo. Results demonstrated that *cyp19a1a* and *cyp19a1b* predominate in ovary and brain respectively, with quantity of both attuned to reproductive cycle. To elucidate estrogen-regulated expression of *cyp19a1b* in brain and *cyp19a1a* in ovary, dose- and time-dependent studies were conducted with estrogen in vitellogenic-stage fish in the presence or absence of specific aromatase inhibitor fadrozole. Results demonstrated that treatment of fish with 17 $\beta$ -estradiol (E2; 1.0  $\mu$ M) for 6 days caused significant upregulation of *cyp19a1b* transcripts, aromatase B protein, and aromatase activity in brain in a dose- and time-dependent manner. Ovarian *cyp19a1a* mRNA, aromatase protein, and aromatase activity, however, was less responsive to E2 than brain. Treatment of fish with an aromatase inhibitor fadrozole for 6 days attenuated both brain and ovarian *cyp19a1* mRNAs expression and stimulatory effects of E2 was also significantly reduced. These results indicate that expression of *cyp19a1b* in brain and *cyp19a1a* in ovary of adult female *A. testudineus* was closely associated to plasma E2 levels and seasonal reproductive cycle. Results further show apparent differential regulation of *cyp19a1a* and *cyp19a1b* expression by E2/fadrozole manipulation.

## KEYWORDS

17 $\beta$ -estradiol, *Anabas testudineus*, *cyp19a1a*, *cyp19a1b*, fadrozole, P450arom genes

## 1 | INTRODUCTION

Aromatization of androgens to estrogens, the key step in estrogen synthesis, is catalyzed by cytochrome P450 aromatase (P450arom), a product of *cyp19a1* gene (for review Simpson & Davis, 2001; Simpson et al., 1994). This enzyme is encoded by a single *cyp19a1* gene in mammals with the exception of pig (Corbin et al., 2009), whereas two distinct genes have been identified in many teleosts. *Cyp19* genes are expressed in gonads, brain, and many other tissues and regulate the location, timing, and quantity of estrogens available for activating

genomic and non-genomic pathways during reproduction and development (Barney, Patil, Gunasekera, & Carter, 2008; Blázquez & Piferrer, 2004; McEwen & Alves, 1999; Roy Moulik et al., 2016; Tchoudakova, Kishida, Wood, & Callard, 2001; Zhao, Dahlman-Wright, & Gustafsson, 2008). Evidence shows that in fish, *cyp19a1a* is involved in ovarian differentiation and development (Blázquez, González, Papadaki, Mylonas, & Piferrer, 2008; Esterhuysen, Heibing, & van Wyk, 2008) and gametogenesis (Ijiri, Kazeto, Lokman, Adachi, & Yamauchi, 2003; Kobayashi et al., 2004), whereas *cyp19a1b* functions in neuroplasticity and neurogenesis (Fortano, Deitcher, Myers, & Bass, 2001). It is now clear that in fish, brain-formed estrogens contribute significantly to the process of sex differentiation, modulation of neuroendocrine function, and sexual behavior (Merchenthaler, Delovade, & Shughrue, 2003; Sawyer,

Abbreviations: E2, estrogen; PRE, preparatory; PRP, pre-spawning; PSP, post-spawning; SP, spawning; T, testosterone